

Blocking rapid ice crystal growth through nonbasal plane adsorption of antifreeze proteins

Luuk L. C. Olijve^{a,b}, Konrad Meister^c, Arthur L. DeVries^d, John G. Duman^e, Shuaiqi Guo^{f,g}, Huib J. Bakker^c, and Ilja K. Voets^{a,b,h,1}

^aInstitute for Complex Molecular Systems, Eindhoven University of Technology, 5600 MB Eindhoven, The Netherlands; ^bLaboratory of Macromolecular and Organic Chemistry, Department of Chemical Engineering and Chemistry, Eindhoven University of Technology, 5600 MB Eindhoven, The Netherlands; ^cInstitute for Atomic and Molecular Physics, Foundation for Fundamental Research on Matter, 1098 XG Amsterdam, The Netherlands; ^dDepartment of Animal Biology, University of Illinois at Urbana–Champaign, Urbana, IL 61801; ^eDepartment of Biological Sciences, University of Notre Dame, Notre Dame, IN 46556; ^fProtein Function Discovery Group, Queen's University, Kingston, ON, Canada K7L 3N6; ^gDepartment of Biomedical and Molecular Sciences, Queen's University, Kingston, ON, Canada K7L 3N6; and ^hLaboratory of Physical Chemistry, Department of Chemical Engineering and Chemistry, Eindhoven University of Technology, 5600 MB Eindhoven, The Netherlands

Edited by Pablo G. Debenedetti, Princeton University, Princeton, NJ, and approved January 26, 2016 (received for review December 14, 2015)

Antifreeze proteins (AFPs) are a unique class of proteins that bind to growing ice crystal surfaces and arrest further ice growth. AFPs have gained a large interest for their use in antifreeze formulations for water-based materials, such as foods, waterborne paints, and organ transplants. Instead of commonly used colligative antifreezes such as salts and alcohols, the advantage of using AFPs as an additive is that they do not alter the physicochemical properties of the water-based material. Here, we report the first comprehensive evaluation of thermal hysteresis (TH) and ice recrystallization inhibition (IRI) activity of all major classes of AFPs using cryoscopy, sonocrystallization, and recrystallization assays. The results show that TH activities determined by cryoscopy and sonocrystallization differ markedly, and that TH and IRI activities are not correlated. The absence of a distinct correlation in antifreeze activity points to a mechanistic difference in ice growth inhibition by the different classes of AFPs: blocking fast ice growth requires rapid nonbasal plane adsorption, whereas basal plane adsorption is only relevant at long annealing times and at small undercooling. These findings clearly demonstrate that biomimetic analogs of antifreeze (glyco)proteins should be tailored to the specific requirements of the targeted application.

antifreeze protein | thermal hysteresis | ice recrystallization inhibition

Ice formation is often detrimental to the structural integrity and performance of materials and processes. The quality of frozen foods deteriorates when large ice crystals form upon prolonged low-temperature storage (1), and the consistency of water-based latex paints is irreversibly destroyed upon partial freezing (2). Also, hypothermic storage effectively extends the preservation period of human organs, although freezing and freeze damage pose a considerable risk (3). Hence, a better understanding of ice crystal growth modifiers could support innovative strategies for cryoprotection, cryopreservation, deicing, and antiicing technologies.

A well-known class of macromolecular ice crystal growth modifiers is antifreeze proteins (AFPs). AFPs enable various freeze-resistant organisms, such as Antarctic fish, to survive in ice-laden habitats at subzero temperatures (4). The efficacy of AFPs in freeze protection is reflected in the wide distribution of AFPs among different biological kingdoms (5–7), and the benefits of their cryoprotective function have already found application in the hypothermic preservation of human blood cells (8) and rat heart transplants (9), in the improvement of the texture of ice cream (10), and in the enhancement of the freeze tolerance of crop plants (11). Unlike their name suggests, AFPs do not prevent freezing in a colligative manner at physiological concentrations. Instead, AFPs recognize embryonic ice crystals in vast excess (55 M) of liquid water and, by binding onto specific crystal planes, prevent further ice growth (12). Based on their origin and structure, AFPs are categorized into different classes, which are illustrated in Fig. 1. Ice-etching assays demonstrate that different

AFPs also target different—sometimes multiple—ice crystal planes, including prism, pyramidal, and basal faces (Fig. 1) (13). Recent Monte Carlo and molecular dynamics simulations confirm this specificity (14–16).

AFPs exhibit two forms of activities. Well known is the thermal hysteresis (TH) activity of AFPs, which is the ability of AFPs to lower the temperature at which existing ice crystals start to grow quickly. This threshold temperature at which “burst growth” occurs is known as the nonequilibrium freezing point. The difference between the melting point and the nonequilibrium freezing point of a solution is defined as TH activity, and is commonly determined by viewing the melting and growth of single ice crystals using a nanoliter cryoscope (17). Antifreeze (glyco)proteins [AF(G)Ps] of fish usually exhibit maximal TH of ~2 °C and are termed moderately active, whereas some insect AFPs can exhibit over ~5 °C of TH and are referred to as hyperactive AFPs (hypAFPs). A unified understanding of the underlying mechanism that causes the large differences in TH is still lacking, but it appears that the targeted ice planes play a crucial role (18).

Another characteristic activity of AFPs is ice recrystallization inhibition (IRI) (19), defined as the visible deceleration of a change in ice texture during an annealing process just below the

Significance

Controlling ice crystal growth is a grand scientific challenge with major technological ramifications. Some cold-adapted organisms such as fish and arthropods are protected against ice growth by producing antifreeze proteins (AFPs). These AFPs adsorb onto embryonic ice crystals, thereby inhibiting their growth. On a macroscopic level, this is evidenced by ice recrystallization inhibition (IRI) and thermal hysteresis (TH) activity. Our research demonstrates the absence of a clear correlation between TH and IRI activities, and underlines the importance of the extent of supercooling and annealing time on the efficacy of AFPs in blocking ice growth. We emphasize that successful application of AFPs and synthetic analogues in innovative strategies for cryoprotection, cryopreservation, and antiicing technologies requires optimization tailored toward the specific purpose.

Author contributions: L.L.C.O., K.M., and I.K.V. designed research; L.L.C.O. and K.M. performed research; A.L.D., J.G.D., and S.G. contributed new reagents/analytic tools; L.L.C.O., K.M., and I.K.V. analyzed data; and L.L.C.O., K.M., A.L.D., H.J.B., and I.K.V. wrote the paper.

The authors declare no conflict of interest.

This article is a PNAS Direct Submission.

Freely available online through the PNAS open access option.

See Commentary on page 3714.

¹To whom correspondence should be addressed. Email: i.voets@tue.nl.

This article contains supporting information online at www.pnas.org/lookup/suppl/doi:10.1073/pnas.1524109113/-DCSupplemental.

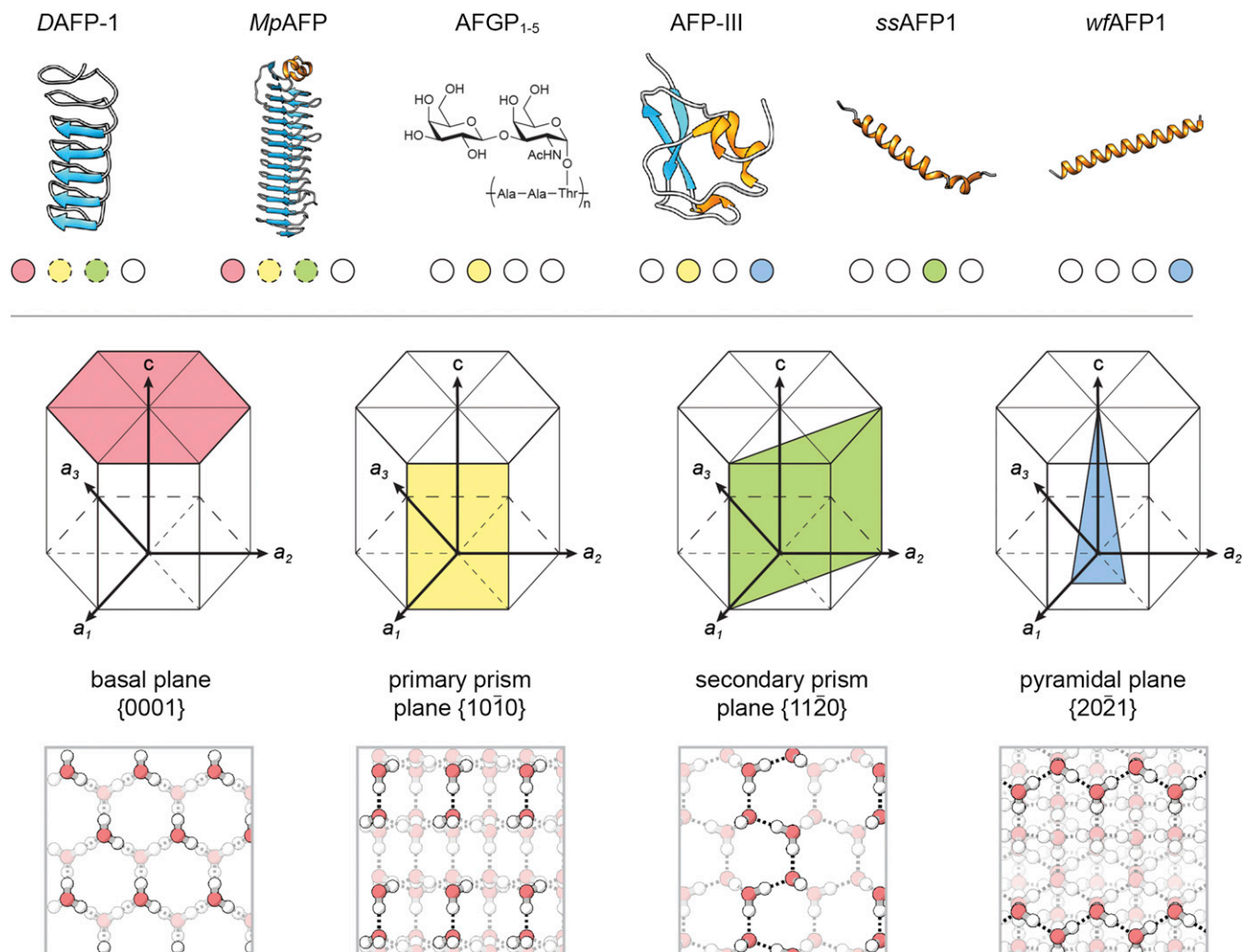


Fig. 1. Overview of antifreeze proteins (AFPs) used in this study and their corresponding ice crystal-binding plane (Top). AFPs are structurally very diverse and are found in a wide variety of organisms (DAFP-1, beetle *Dendroides canadensis*; MpAFP, Antarctic bacterium *M. primoryensis*; AFGP₁₋₅, various species of Antarctic Notothenioid fishes; AFP-III, ocean pout fish; ssAFP1, shorthorn sculpin fish; wfAFP1, winter flounder fish). Virtually all natural ice on Earth is hexagonal ice (Ih). The AFPs adsorb to different ice planes, such as the slow-growing basal plane and the faster-growing prismatic fronts (Middle). The distinct growth rates appear to be correlated with the extent of the hydrogen-bonded water molecular network on the surface of the ice planes, as illustrated in the cartoon (Bottom). Red spheres represent oxygen atoms, white spheres represent hydrogen atoms, and dashed lines indicate hydrogen bonding.

melting temperature of the sample (20–22). Recrystallization of ice involves ice grain boundary migration (20), in which large ice crystals increase in size and small crystals disappear (i.e., Ostwald ripening). AFPs inhibit grain boundary migration processes by stopping ice from growing and melting at the boundaries (23, 24). IRI is already significant at submicromolar AFP concentrations, which is well below concentrations required for TH (25). As a result of IRI, ice crystals remain small in frozen solutions, which is essential for survival in the cold and the preservation of frozen foods and other frozen hydrated materials (26).

Despite great progress in understanding TH and IRI activity of AFPs, the relation between these activities is still highly debated (27–30). Nonetheless, visual examination of crystals in the presence of AFPs (31, 32) as well as ice etching (13) showed that direct ice binding plays a crucial role in both types of activity. Further exploitation of ice crystal growth modulation by macromolecular antifreezes in industrial applications may lead to the development of inexpensive synthetic materials that can enhance or outperform their natural counterparts (33). However, rational design of such materials can only be achieved if the underlying antifreeze function of AFPs is completely understood. It is

essential to understand if and how IRI and TH activities are related to each other and the differential affinity for their various ice crystal planes.

We investigated all major classes of AFPs using nanoliter cryoscopy, sonocrystallization, and IRI activity assays. Nanoliter cryoscopy is the most commonly used method to measure the TH activity of AFPs (17). In cryoscopy, a nanoliter aqueous sample droplet is directly observed under a microscope (Fig. S1). A sample solution is first flash-frozen and then melted back until a small single ice crystal is obtained. Samples are then further cooled at a very slow rate, until a sudden burst of ice growth is observed. The TH determined in this manner is defined as the difference between the melting point and the nonequilibrium freezing point, which is the temperature at which ice starts to grow in a sudden burst. The major advantage of nanoliter cryoscopy is that a single measurement requires only several nanoliters of AFP solution. However, factors such as cooling and melting rate, annealing time, and initial crystal size affect the determination of the TH activity (34). To overcome these limitations, Gaede-Koehler et al. developed a highly accurate, time-independent method based on sonocrystallization to determine

TH activity (Fig. S2) (35). In sonocrystallization, a sample solution is slowly supercooled by approximately -6°C , followed by a short ultrasound pulse resulting in nucleation and freezing. Slow melting of the sample allows for the determination of the freezing and melting points within a single experiment. The sonocrystallization method provides control of the degree of supercooling and rate of freezing, excludes any observer-based bias, and is independent of initial ice crystal size. IRI activity is determined quantitatively as the threshold concentration below which ice crystal growth is apparent in a thin wafer of sample solution in consecutive polarized optical microscopy images taken at regular time intervals (Fig. S3).

Our results show a significant difference in TH activity measured by nanoliter cryoscopy and sonocrystallization. TH activity measured by cryoscopy is the highest for AFPs that bind to basal (and other) planes, whereas nonbasal plane binding is essential to demonstrate hysteresis activity using sonocrystallization. This apparent contradiction is due to the longer exposure time of nascent ice crystals to AFPs at a lower ice volume fraction in cryoscopy compared with sonocrystallization. The adsorption kinetics of AFPs also impacts TH activity and is known to depend on both AFP type and the ice plane of adsorption (36, 37). Furthermore, no significant correlation is found between TH and IRI activities. These insights provide a deeper understanding of how AFPs arrest ice crystal growth, and emphasize that successful application of antifreeze (glyco)proteins and synthetic analogs in processes and technologies relies on a optimization tailored to the targeted application.

Results

Freezing Point Determination Using the Sonocrystallization Method.

Fig. 2 shows a typical sonocrystallization measurement of an aqueous solution of the recombinantly expressed quaternary-amino-ethyl (QAE)-binding isoform of AFP-III from ocean

pout (rQAE). After initiation of ice nucleation by a short ultrasound pulse, latent heat is released, followed by the development of a stable freezing plateau. Slow melting of the sample allows determination of the melting point, and thus the TH gap (Fig. 2B), with high reproducibility (Fig. S2). The TH activity of recombinant rQAE and AFP-III from a natural source (*op*AFP-III) is proportional to the square root of the molar concentration (Fig. 2C), which is in accordance with cryoscopy data (38). The rQAE is slightly more active than *op*AFP-III due to the presence of inactive isoforms in the purified extract of the latter. We further determined the activity of rQAE mutants, proving that single mutations within the ice-binding site of the protein can have a marked impact on the TH activity, which underlines the delicate balance between the structure and activity of AFPs (Fig. S4).

Activity Ranking Based on Cryoscopy and Sonocrystallization Experiments.

Table 1 shows the TH activities of six different AFPs obtained by nanoliter cryoscopy and sonocrystallization. The six AFPs vary significantly in terms of structure, putative ice-binding plane, and TH activity. In cryoscopy, the basal plane-binding AFPs from *M. primoryensis* (*Mp*AFP) and *Dendroides canadensis* (*DAFP*-1) show the highest maximum activities (TH = $5\text{--}6^{\circ}\text{C}$), as expected. Fish type I and III AFPs show comparable maximal activities with, for instance, TH = 0.6°C for *wf*AFP1 from winter flounder and rQAE at 5 mg/mL and 3 mg/mL, respectively. These values are consistent with previously reported values for these proteins (38, 47). Surprisingly, in sonocrystallization, the fish AFPs show TH $\leq 0.5^{\circ}\text{C}$, whereas basal plane-binding AFPs of nonfish exhibit TH $\leq 0.2^{\circ}\text{C}$ (Fig. S5).

To directly compare the values for the TH activity from the two methods, we have determined the ratio TH/\sqrt{C} corresponding to the slope of the linear relation between TH and the square root of the protein concentration as shown in Fig. 2C and Fig. S6.

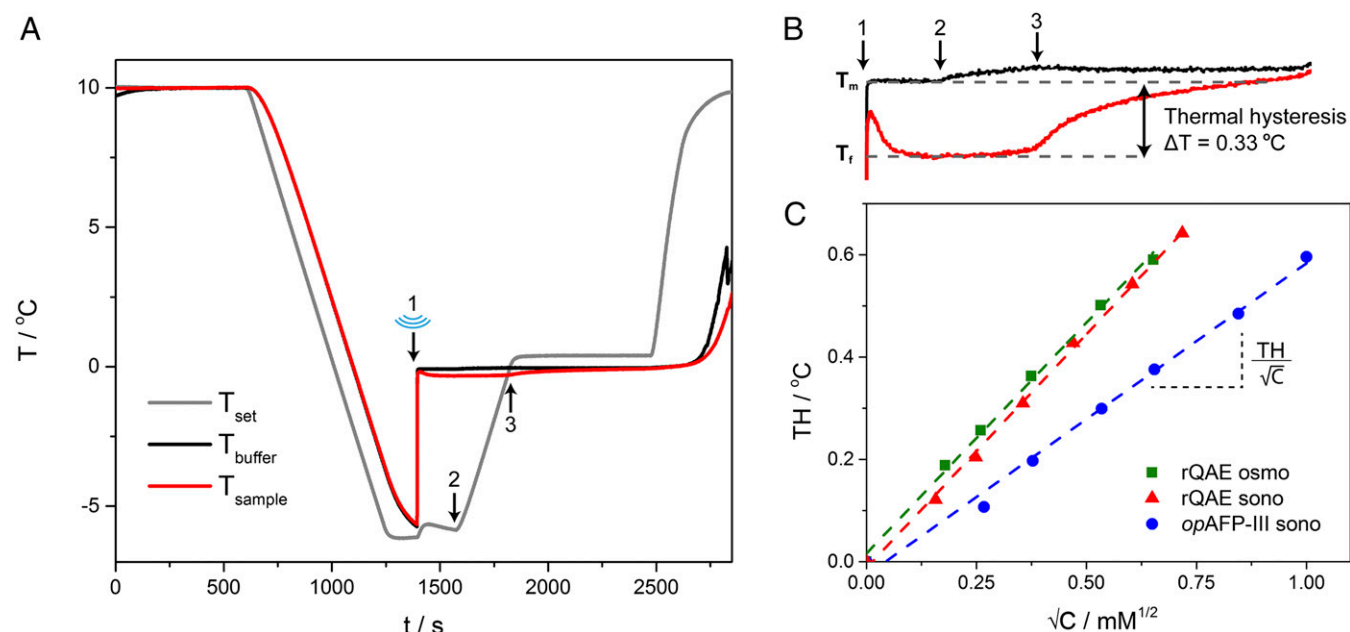


Fig. 2. (A) Sonocrystallization measurement of the TH activity of recombinant type III AFP (rQAE, 1 mg/mL). The bold numbers indicate (1) application of the ultrasound pulse, (2) onset of heating, and (3) cross-point where the set temperature passes the nonequilibrium freezing point of the sample. (B) Zoom-in of A, showing the development of freezing (T_f) and melting (T_m) plateaus. TH is defined as the difference between the freezing point plateau of the buffer solution and the nonequilibrium freezing point of the AFP solution. The slight increase in temperature ($\sim 0.03^{\circ}\text{C}$) of the buffer at point 2 is due to infrared irradiation from the heating unit after the onset of heating. (C) TH measurements of 0.025- to 1.0-mM solutions of type III AFP in cryoscopy [green square (38)] and sonocrystallization (red triangle and blue circle). The rQAE is the recombinantly expressed QAE isoform (HPLC-12), and *op*AFP-III is from natural source (AF Protein Inc.), which is a mixture of different isoforms. All samples were measured in 20 mM Tris, pH 7.5. The slope of the linear relation between TH and C gives the ratio TH/\sqrt{C} and is used as a measure to directly compare AFP activity of sonocrystallization with nanoliter cryoscopy.

Table 1. TH and IRI activity of AFPs from nanoliter cryoscopy, sonocrystallization, and optical microscopy measurements

AFP	Ice crystal-binding plane	TH_{nano}/\sqrt{C} , °C·mM ^{-1/2}	TH_{sono}/\sqrt{C} , °C·mM ^{-1/2}	C_i , μM
rQAE	{10 $\bar{1}$ 0} primary prism and {20 $\bar{2}$ 1} pyramidal planes (39)	0.90	0.91	5.9
AFGP ₁₋₅	{10 $\bar{1}$ 0} primary prism planes (40, 41)	0.78	0.48	0.00091
<i>Mp</i> AFP	prism and basal planes (42)	20.8	0.85	0.011
<i>DAFP</i> -1	prism and basal planes (43)	19.8	0.32	2.1
<i>ss</i> AFP1	{11 $\bar{2}$ 0} secondary prism planes (13)	0.57	0.13	n.d.
<i>wf</i> AFP1	{20 $\bar{2}$ 1} pyramidal planes (13)	0.48	0.07	5.8

The ratio TH/\sqrt{C} is used as a quantitative measure of TH activity. It corresponds to the slope of the curve that describes TH as a function of the square root of the protein concentration as illustrated in Fig. 2C. C_i is the IRI efficacy and represents the inhibitor concentration determined from the inflection point of a curve of the recrystallization constant k_d vs. C_{AFP} (Fig. S7) (21, 22). The tabulated cryoscopy values are from this work for rQAE, AFGP₁₋₅, and *DAFP*-1 and from literature for *wf*AFP1 (44), *Mp*AFP (45), and *ss*AFP1 (46). Boldfaced show the two AFPs with the highest measured activity for a particular activity assay.

This reflects the efficiency of the AFPs rather than their efficacy (i.e., maximal activity). Ordering AFPs based on cryoscopy from the most to the least active gives *Mp*AFP (20.8) > *DAFP*-1 (19.8) > rQAE (0.90) > AFGP₁₋₅ (0.78) > *ss*AFP1 (0.57) > *wf*AFP1 (0.48). The ranking based on sonocrystallization is entirely different: rQAE (0.91) > *Mp*AFP (0.85) > AFGP₁₋₅ (0.48) > *DAFP*-1 (0.32) > *ss*AFP1 (0.13) > *wf*AFP1 (0.07). Remarkably, rQAE is the most active AFP in the sonocrystallization assay with $TH_{sono}/\sqrt{C} \approx TH_{nano}/\sqrt{C}$. *Mp*AFP is 25 times less active in sonocrystallization and shows only a small TH gap in sonocrystallization (Fig. S5C). Also, *DAFP*-1 (0.32) displays a dramatic 62-fold decrease in activity. The small α -helical proteins *ss*AFP1 (0.13) and *wf*AFP1 (0.07) show only minimal activity in a sonocrystallization assay (Fig. S5 E and F).

Out of all investigated AFPs, only AFP-III and AFGP₁₋₅ show a comparable TH activity in cryoscopy and sonocrystallization. Interestingly, ice etching revealed that both these proteins bind predominantly to the six equivalent {10 $\bar{1}$ 0} primary prism planes (Fig. 1 and Table 1). Ice etching studies on type I AFPs demonstrated binding of *wf*AFP1 to the 12 equivalent {20 $\bar{2}$ 1} pyramidal planes and *ss*AFP1 to the six equivalent {11 $\bar{2}$ 0} secondary prism planes. Most striking is the poor performance of the insect and bacterial AFPs in sonocrystallization, even though these proteins have been reported to bind both prism and basal planes. This dual recognition is thought to be the basis for their high activity in cryoscopy (18, 48).

Correlation Between IRI and TH Activities. All investigated AFPs with confirmed TH activity show IRI activity at low (micromolar) concentrations, from which we have determined the IRI efficacy (C_i), which represents the effective AFP concentration below which no IRI activity is observed (Table 1 and Fig. S7). The measured C_i for rQAE = 5.9 μM, *wf*AFP1 = 5.8 μM, and AFGP₁₋₅ = 0.00091 μM in this work are similar to values reported by Budke et al.: natural AFP-III = 0.49 μM, natural AFP-I variant S35 = 6.1 μM, and natural AFGP1-5 = 0.001 μM (22). The difference between C_i of rQAE in our study and natural AFP-III in the study of Budke et al. may be ascribed to a difference in protein purity of the natural extract.

Strikingly, the IRI experiments yield the highest IRI activity for AFGP₁₋₅, whereas only moderate TH activity is observed for AFGP₁₋₅ in both cryoscopy and sonocrystallization. The hyperactive *DAFP*-1 with 20- to 40-fold higher TH_{nano}/\sqrt{C} activities than rQAE and *wf*AFP1 shows only moderate IRI activity. This contradictory observation has also been noted by other groups (27, 28). We have calculated the Pearson correlation coefficient (ρ) of the TH and IRI activity parameters determined from the sonocrystallization (TH_{sono}/\sqrt{C}), nanoliter cryoscopy (TH_{nano}/\sqrt{C}), and IRI (C_i) experiments, but found no significant correlation (Table S1).

Discussion

In this study, we report nanoliter cryoscopy, sonocrystallization, and ice recrystallization inhibition experiments on all major classes of AFPs to investigate the factors that govern both TH and IRI activity. Using TH/\sqrt{C} as a quantitative measure for TH activity, we have ranked AFPs by sonocrystallization to rQAE > *Mp*AFP > AFGP₁₋₅ > *DAFP*-1 > *ss*AFP1 > *wf*AFP1, which differs significantly from the ranking based on cryoscopy, in which *Mp*AFP and *DAFP*-1 are by far the most active. It seems that all AFPs that bind prismatic planes (rQAE, AFGP₁₋₅, *Mp*AFP, and *DAFP*-1) give a significant noncolligative freezing point depression in sonocrystallization; these are ranked one through four out of six. AFPs that solely target the secondary prism (*ss*AFP1) or pyramidal planes (*wf*AFP1) show, on molar basis, very little activity. Surprisingly, “hyperactive” AFPs perform poorly in sonocrystallization, with a 25-fold (*Mp*AFP) and 62-fold (*DAFP*-1) lower TH_{sono}/\sqrt{C} , which is even lower than the activity of the “moderate” rQAE. Adsorption of hyperactive AFPs onto both prism and basal planes has been suggested to enhance their ability to depress the nonequilibrium freezing point, making them more potent than their moderately active counterparts that target a single, nonbasal ice crystal plane (18). Our findings clearly demonstrate that primary prism plane binding is a far more important determinant of TH_{sono}/\sqrt{C} than basal plane binding.

This raises the question: why are hyperactive AFPs potent in cryoscopy yet inefficient in sonocrystallization? We propose that the binding of the hyperactive AFPs to basal planes is less relevant in the sonocrystallization experiments, because blocking ice growth along the fast ice growth *a*-axis direction is more important. The initiation of ice crystallization in a sonocrystallization assay results from many nucleation sites, and ice growth is very fast because the sample is significantly undercooled. The most favorable and fastest growing ice lattice direction is along the *a*-axis direction {11 $\bar{2}$ 0} (13, 49). Therefore, binding to prism planes is crucial, as only adsorption onto this plane blocks the predominant growth mode. Ice grows fastest along the *a*-axis direction, because here, chains or networks of water molecules can cooperatively hydrogen bond to the ice lattice, having one hydrogen bond per water molecule to attach to the ice surface. The frontal views of the specific ice crystal planes depicted in Fig. 1 illustrate how the extensive hydrogen-bonding network of the water molecules in the ice lattice favors the attachment of new water molecules. Ice grows fast, but less fast, along the {10 $\bar{1}$ 0} direction because only pairs of water molecules can attach here, having one hydrogen bond per two water molecules interact with the ice surface. Ice growth along the *c* axis requires 2D nucleation on the molecularly smooth basal plane, which makes ice growth there slow. HypAFP adsorption onto the slowly growing basal planes is thus irrelevant at moderate undercooling when rapid ice growth proceeds mainly by attachment at the prism planes.

Fluorescent microscopy studies showed that hypAFPs adsorb to both prism and basal planes; however, little is known about the difference in surface coverage (50). A complete arrest of ice growth requires a sufficiently high surface coverage, which is attainable if the rate of AFP adsorption (which is directly related to the AFP concentration in solution) is fast compared with the growth rate of the ice crystal plane (37). If the AFP concentration and/or the AFP adsorption rate are too low, ice-bound proteins will get engulfed. A recent fluorescence study by Drori et al. reports similar adsorption rates for rQAE and *Tm*AFP (a structural analog of *DAFP*-1) at the prism plane (36); however, *Tm*AFP adsorption at the basal plane was much slower. Relatively slow hypAFP adsorption at the basal planes only becomes relevant during prolonged annealing at minor supercooling and thus modest ice growth rates. The high values for TH in nanoliter cryoscopy assays arise due to long exposure times at slow cooling rates and modest supercooling, which accommodates slow hypAFP adsorption onto basal planes. By contrast, ice growth is very rapid during a sonocrystallization experiment at several degrees of supercooling, which warrants fast and significant AFP accumulation at the prismatic planes to arrest ice growth. Apparently, rQAE accumulates with a high adsorption rate at sufficient coverage on the primary prism planes to block rapid growth in sonocrystallization experiments, giving rise to a similar TH_{sono}/\sqrt{C} and TH_{nano}/\sqrt{C} , which is unique for rQAE.

A unified theory to describe how structurally different AFPs accommodate TH activity thus needs to take the following factors into account: (i) ice-binding plane of AFP, (ii) ice adsorption rate of the AFP, (iii) surface coverage, (iv) degree of undercooling or cooling rate (and thus speed of ice growth), and (v) kinetics and mechanism of ice nucleation (51, 52). Because all these factors are different in sonocrystallization and cryoscopy for the various AFPs, no significant correlation is observed. Furthermore, the degree of undercooling can significantly change the antifreeze properties of the AFP. Feeney and coworkers reported that AFGP₈ shows only a freezing point depression when freezing is initiated after modest supercooling (−1 °C), which is absent when frozen after deep supercooling (−6 °C) (53, 54). The loss of AFGP₈ activity was hypothesized to be related to differences in the structure of the ice crystal planes. If the ice surface is “rough” due to imperfections in the ice crystal planes, as is the case if ice is made at −6 °C, the energy requirement for ice growth is low. If the ice surface is smooth, ice growth depends on surface nucleation to form a new ice crystal layer. Unraveling the relative importance of these factors warrants detailed physico-chemical experiments (single-molecule imaging, force spectroscopy, sum frequency generation spectroscopy on the ice/water interface, etc.) and accurate (molecular dynamics) simulations (55–57).

In conclusion, the TH and IRI activity of AFPs as determined by cryoscopy, sonocrystallization, and optical microscopy are not

correlated due to differences in ice adsorption behavior and operating conditions. These differential activities highlight the strength and weakness of the different AFPs related to their biological role. For example, the hypAFPs produced by insects need to block ice growth when temperatures drop far below 0 °C (i.e., large TH under slow cooling conditions). On the other hand, fish living in polar sea water with only modest temperature variations require rapid ice blocking and very effective IRI activity, as the AFP-stabilized ice crystals remain in their body fluids throughout their lifespan because the endogenous ice crystals do not melt at warmer temperatures in summer (58). These findings demonstrate that the application of AFPs and synthetic analogs requires a tailored optimization to the specific purpose. Especially, rational design strategies for synthetic ice binders should not focus on compatibility with all ice crystal planes, but, instead, factors such as cooling rate, extent of undercooling, annealing times, etc., of the intended application need to be taken into account. Furthermore, we propose abandonment of the categorization of AFPs into moderate and hyperactive variants, as this is based on an activity ranking that is method- and protocol-dependent. These new insights provide a deeper understanding of the underlying mechanism that governs IRI and TH activity, which supports the development of synthetic macromolecular antifreezes for cryoprotection, cryopreservation, deicing, and antiicing technologies.

Materials and Methods

Protein Samples. Recombinant expression and purification of rQAE (55), *DAFP*-1 (59), and *Mp*AFP (42) was performed as described previously. The *wf*AFP1 was synthesized using solid-phase peptide synthesis as described previously (60). The *ss*AFP1 and AFGP_{1–5} were purified from shorthorn sculpin and Antarctic tooth fish blood serum by gel filtration chromatography. The *op*AFP-III was purchased from A/F Protein Inc. and used without further purification. All other chemicals were purchased from Sigma Aldrich and used as received.

TH and IRI Experiments. The Clifton nanoliter cryoscopy (44), sonocrystallization (55), and IRI (21, 22) experiments were performed as described elsewhere. All samples were measured in 20 mM Tris, pH 7.5 buffer, except *Mp*AFP, which was measured in 20 mM Tris, 2 mM CaCl₂, pH 7.5 buffer.

ACKNOWLEDGMENTS. We acknowledge Harrie de Laat, Hans Wijtvlit, and Meindert Janszen of the Engineering and Prototyping Center of Eindhoven University for their work on the sonocrystallization setup, Luuk van Schijndel for his work on preliminary sonocrystallization experiments, Ralph Bosmans for his help with the Q-TOF mass spectroscopy measurements, Tim van der Steen and Koen Pieterse of the ICMS Animation Studio for designing Fig. 1, and Prof. Peter Davies for proofreading the manuscript. This work is financially supported by NWO (Veni Grant 700.10.406) and the European Union (FP7-PEOPLE-2011-CIG Contract 293788 and ERC-2014-StG Contract 635928). K.M. acknowledges the European Commission for funding through the award of a Marie Curie fellowship.

- Petzold G, Aguilera JM (2009) Ice morphology: Fundamentals and technological applications in foods. *Food Biophys* 4(4):378–396.
- Zhao C-L, et al. (2006) Direct observation of freeze-thaw instability of latex coatings via high pressure freezing and cryogenic SEM. *JCT Res* 3(2):109–115.
- Berendsen TA, et al. (2014) Supercooling enables long-term transplantation survival following 4 days of liver preservation. *Nat Med* 20(7):790–793.
- DeVries AL, Wohlschlag DE (1969) Freezing resistance in some Antarctic fishes. *Science* 163(3871):1073–1075.
- Fletcher GL, Hew CL, Davies PL (2001) Antifreeze proteins of teleost fishes. *Annu Rev Physiol* 63(1):359–390.
- Duman JG (2001) Antifreeze and ice nucleator proteins in terrestrial arthropods. *Annu Rev Physiol* 63(1):327–357.
- Davies PL (2014) Ice-binding proteins: A remarkable diversity of structures for stopping and starting ice growth. *Trends Biochem Sci* 39(11):548–555.
- Deller RC, Vatsish M, Mitchell DA, Gibson MI (2014) Synthetic polymers enable non-vitreous cellular cryopreservation by reducing ice crystal growth during thawing. *Nat Commun* 5:3244.
- Amir G, et al. (2004) Prolonged 24-hour subzero preservation of heterotopically transplanted rat hearts using antifreeze proteins derived from arctic fish. *Ann Thorac Surg* 77(5):1648–1655.
- Regand A, Goff HD (2006) Ice recrystallization inhibition in ice cream as affected by ice structuring proteins from winter wheat grass. *J Dairy Sci* 89(1):49–57.
- Worrall D, et al. (1998) A carrot leucine-rich-repeat protein that inhibits ice recrystallization. *Science* 282(5386):115–117.
- Sharp KA (2014) The remarkable hydration of the antifreeze protein Maxi: A computational study. *J Chem Phys* 141(22):22D510.
- Knight CA, Cheng CC, DeVries AL (1991) Adsorption of alpha-helical antifreeze peptides on specific ice crystal surface planes. *Biophys J* 59(2):409–418.
- Nutt DR, Smith JC (2008) Dual function of the hydration layer around an antifreeze protein revealed by atomistic molecular dynamics simulations. *J Am Chem Soc* 130(39):13066–13073.
- Dalal P, Sönnichsen FD (2000) Source of the ice-binding specificity of antifreeze protein type I. *J Chem Inf Comput Sci* 40(5):1276–1284.
- Wierzbicki A, et al. (2007) Antifreeze proteins at the ice/water interface: Three calculated discriminating properties for orientation of type I proteins. *Biophys J* 93(5):1442–1451.
- Knight CA, DeVries AL, Oolman LD (1984) Fish antifreeze protein and the freezing and recrystallization of ice. *Nature* 308(5956):295–296.
- Scotter AJ, et al. (2006) The basis for hyperactivity of antifreeze proteins. *Cryobiology* 53(2):229–239.

19. Capicciotti CJ, Doshi M, Ben RN (2013) *Ice Recrystallization Inhibitors: From Biological Antifreezes to Small Molecules* (INTECH Open Access, Rijeka, Croatia).
20. Knight CA, Duman JG (1986) Inhibition of recrystallization of ice by insect thermal hysteresis proteins: A possible cryoprotective role. *Cryobiology* 23(3):256–262.
21. Budke C, Heggemann C, Koch M, Sewald N, Koop T (2009) Ice recrystallization kinetics in the presence of synthetic antifreeze glycoprotein analogues using the framework of LSW theory. *J Phys Chem B* 113(9):2865–2873.
22. Budke C, et al. (2014) Quantitative efficacy classification of ice recrystallization inhibition agents. *Cryst Growth Des* 14(9):4285–4294.
23. Knight CA, Hallett J, DeVries AL (1988) Solute effects on ice recrystallization: An assessment technique. *Cryobiology* 25(1):55–60.
24. Knight CA, Wen D, Laursen RA (1995) Nonequilibrium antifreeze peptides and the recrystallization of ice. *Cryobiology* 32(1):23–34.
25. Tomczak MM, Marshall CB, Gilbert JA, Davies PL (2003) A facile method for determining ice recrystallization inhibition by antifreeze proteins. *Biochem Biophys Res Commun* 311(4):1041–1046.
26. Venketesh S, Dayananda C (2008) Properties, potentials, and prospects of antifreeze proteins. *Crit Rev Biotechnol* 28(1):57–82.
27. Yu SO, et al. (2010) Ice restructuring inhibition activities in antifreeze proteins with distinct differences in thermal hysteresis. *Cryobiology* 61(3):327–334.
28. Capicciotti CJ, Poisson JS, Boddy CN, Ben RN (2015) Modulation of antifreeze activity and the effect upon post-thaw HepG2 cell viability after cryopreservation. *Cryobiology* 70(2):79–89.
29. Sidebottom C, et al. (2000) Heat-stable antifreeze protein from grass. *Nature* 406(6793):256.
30. Singh P, Hanada Y, Singh SM, Tsuda S (2014) Antifreeze protein activity in Arctic cryoconite bacteria. *FEMS Microbiol Lett* 351(1):14–22.
31. Pertaya N, et al. (2007) Growth–melt asymmetry in ice crystals under the influence of spruce budworm antifreeze protein. *J Phys Condens Matter* 19(41):412101.
32. Celik Y, et al. (2013) Microfluidic experiments reveal that antifreeze proteins bound to ice crystals suffice to prevent their growth. *Proc Natl Acad Sci USA* 110(4):1309–1314.
33. Gibson MI (2010) Slowing the growth of ice with synthetic macromolecules: Beyond antifreeze (glyco) proteins. *Polym Chem* 1(8):1141–1152.
34. Takamichi M, Nishimiya Y, Miura A, Tsuda S (2007) Effect of annealing time of an ice crystal on the activity of type III antifreeze protein. *FEBS J* 274(24):6469–6476.
35. Gaede-Koehler A, Kreider A, Canfield P, Kleemeier M, Grunwald I (2012) Direct measurement of the thermal hysteresis of antifreeze proteins (AFPs) using sonocrystallization. *Anal Chem* 84(23):10229–10235.
36. Drori R, Celik Y, Davies PL, Braslavsky I (2014) Ice-binding proteins that accumulate on different ice crystal planes produce distinct thermal hysteresis dynamics. *J R Soc Interface* 11(98):20140526.
37. Knight CA, DeVries AL (2009) Ice growth in supercooled solutions of a biological “antifreeze”, AFP-1: An explanation in terms of adsorption rate for the concentration dependence of the freezing point. *Phys Chem Chem Phys* 11(27):5749–5761.
38. Baardsnes J, Davies PL (2002) Contribution of hydrophobic residues to ice binding by fish type III antifreeze protein. *Biochim Biophys Acta. Proteins Proteomics* 1601(1):49–54.
39. Antson AA, et al. (2001) Understanding the mechanism of ice binding by type III antifreeze proteins. *J Mol Biol* 305(4):875–889.
40. Raymond JA, Wilson P, DeVries AL (1989) Inhibition of growth of nonbasal planes in ice by fish antifreezes. *Proc Natl Acad Sci USA* 86(3):881–885.
41. Wilson PW, Beaglehole D, DeVries AL (1993) Antifreeze glycopeptide adsorption on single crystal ice surfaces using ellipsometry. *Biophys J* 64(6):1878–1884.
42. Garnham CP, Campbell RL, Davies PL (2011) Anchored clathrate waters bind antifreeze proteins to ice. *Proc Natl Acad Sci USA* 108(18):7363–7367.
43. Liou Y-C, Tocilj A, Davies PL, Jia Z (2000) Mimicry of ice structure by surface hydroxyls and water of a β -helix antifreeze protein. *Nature* 406(6793):322–324.
44. Meister K, et al. (2014) The role of sulfates on antifreeze protein activity. *J Phys Chem B* 118(28):7920–7924.
45. Garnham CP, et al. (2008) A Ca²⁺-dependent bacterial antifreeze protein domain has a novel beta-helical ice-binding fold. *Biochem J* 411(1):171–180.
46. Baardsnes J, et al. (2001) Antifreeze protein from shorthorn sculpin: Identification of the ice-binding surface. *Protein Sci* 10(12):2566–2576.
47. Chao H, et al. (1997) A diminished role for hydrogen bonds in antifreeze protein binding to ice. *Biochemistry* 36(48):14652–14660.
48. Bar-Dolev M, Celik Y, Wettlaufer JS, Davies PL, Braslavsky I (2012) New insights into ice growth and melting modifications by antifreeze proteins. *J R Soc Interface* 9(77):3249–3259.
49. Hobbs PV (1974) *Ice Physics* (Clarendon, Oxford).
50. Drori R, Davies PL, Braslavsky I (2015) Experimental correlation between thermal hysteresis activity and the distance between antifreeze proteins on an ice surface. *RSC Advances* 5(11):7848–7853.
51. Haji-Akbari A, Osterday KE, Heneghan AF, Haymet ADJ (2010) Type I antifreeze proteins enhance ice nucleation above certain concentrations. *J Biol Chem* 285(45):34741–34745.
52. Hazi-Akbari A, DeBenedetti PG (2015) Direct calculation of ice homogeneous nucleation rate for a molecular model of water. *Proc Natl Acad Sci USA* 112(34):10582–10588.
53. Feeney RE, Burcham TS, Yeh Y (1986) Antifreeze glycoproteins from polar fish blood. *Annu Rev Biophys Chem* 15(1):59–78.
54. Burcham TS, Knauf MJ, Osuga DT, Feeney RE, Yeh Y (1984) Antifreeze glycoproteins: Influence of polymer length and ice crystal habit on activity. *Biopolymers* 23(7):1379–1395.
55. Meister K, et al. (2014) Observation of ice-like water layers at an aqueous protein surface. *Proc Natl Acad Sci USA* 111(50):17732–17736.
56. Oude Vrielink AS, Aloï A, Olijve LLC, Voets IK (2016) Interaction of ice binding proteins with ice, water and ions. *Biointerphases* 11(1):018906.
57. Todde G, Hovmöller S, Laaksonen A (2015) Influence of antifreeze proteins on the ice/water interface. *J Phys Chem B* 119(8):3407–3413.
58. Cziko PA, DeVries AL, Evans CW, Cheng C-HC (2014) Antifreeze protein-induced superheating of ice inside Antarctic notothenioid fishes inhibits melting during summer warming. *Proc Natl Acad Sci USA* 111(40):14583–14588.
59. Amornwittawat N, Wang S, Duman JG, Wen X (2008) Polycarboxylates enhance beetle antifreeze protein activity. *Biochim Biophys Acta Proteins Proteomics* 1784(12):1942–1948.
60. Lotze S, et al. (2015) Communication: Probing the absolute configuration of chiral molecules at aqueous interfaces. *J Chem Phys* 143(20):201101.
61. Xiao N, et al. (2010) Comparison of functional properties of two fungal antifreeze proteins from *Antarctomyces psychrotrophicus* and *Typhula ishikariensis*. *FEBS J* 277(2):394–403.
62. Granham CP, et al. (2010) Compound ice-binding site of an antifreeze protein revealed by mutagenesis and fluorescent tagging. *Biochemistry* 49(42):9063–9071.
63. Howard EI, et al. (2011) Neutron structure of type-III antifreeze protein allows the reconstruction of AFP–ice interface. *J Mol Recognit* 24(4):724–732.